AD-A175 460 HIGH-SPEED PULSE PROPAGATION IN INTEGRATED CIRCUITS(U) 1/1
TUFTS UNIV MEDFORD MA DEPT OF ELECTRICAL ENGINEERING
D PREIS 31 OCT 86 ARO-21214 2L-EL DAAG29-84-K-0188
UNCLASSIFIED F/G 9/5 NL

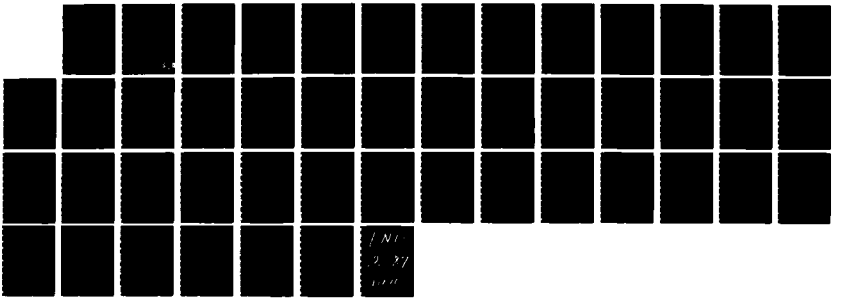

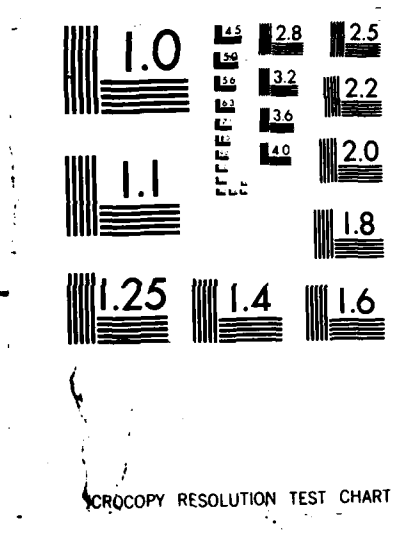
1.0
1.1
1.25
1.4
1.6
1.8
2.0
2.2
2.5
2.8
3.2
3.6
4.0
4.5
5.0
5.6
6.3
7.1
8.0
9.0
MICROCOPY RESOLUTION TEST CHART

8c. ADDRESS (City, State, and ZIP Code)	10. SOURCE OF FUNDING NUMBERS			
P. O. Box 12211 Research Triangle Park, NC 27709-2211	PROGRAM ELEMENT NO.	PROJECT NO.	TASK NO.	WORK UNIT ACCESSION NO.

11. TITLE (Include Security Classification)

High-Speed Pulse Propagation in Integrated Circuits (Unclassified)

12 PERSONAL AUTHOR(S) Dr. D. Preis, Associate Professor of Electrical Engineering

13a. TYPE OF REPORT	13b. TIME COVERED	14. DATE OF REPORT (Year, Month, Day)	15. PAGE COUNT
Final	FROM 9/1/84 TO 8/31/86	1986 October 31	45

16. SUPPLEMENTARY NOTATION

The view, opinions and/or findings contained in this report are those of the author(s) and should not be construed as an official Department of the Army position, policy, or decision, unless so designated by other documentation.

17. COSATI CODES			18. SUBJECT TERMS (Continue on reverse if necessary and identify by block number)
FIELD	GROUP	SUB-GROUP	VHSIC, Interconnects, distributed circuits, pulse propagation, time-domain analysis, coupling, crosstalk, interference, matching, nominal resistance, EMP, reflection coefficient, surface waves, lateral waves.

ARO 21214.2-EL

"High-Speed Pulse Propagation in Integrated Circuits"

Final Technical Report

D. Preis, Ph.D.
Associate Professor of
Electrical Engineering

31 October 1986
U. S. Army Research Office

Contract Number DAAG 29-84-k-0188
Tufts University
Medford, MA 02155

Approved for Public Release;
Distribution Unlimited

Accession For	
NTIS GRA&I	☒
DTIC TAB	☐
Unannounced	☐
Justification	
By	
Distribution/	
Availability Codes	
Dist	Avail and/or Special
A-1	

Table of Contents

1. Introduction and Overview

The subject of this report is the characterization and interaction of signal paths in very-high-speed integrated circuits. A long-range objective of research on this problem is optimization of signal propagation to increase operating speed and minimization of both internal and external interference. This can be accomplished by developing suitable theoretical models for the physical phenomena involved. These models are based on circuit theory and linear system theory, distributed circuits and transmission-line theory, and field-theoretic considerations. Several new and interesting results are reported here and many new useful formulas given.

First, the signal path is modelled as a distributed circuit and the propagating waves of voltage, current, and power flow (as a function of time and position along the path) are evaluated analytically for increasingly complicated, but more accurate, path models. Then the problem of matching the input voltage pulse shape to the path or, conversely, the path impedance to the pulse shape is considered. This leads to the new concept of nominal resistance and a simple way to predict peak possible path currents. Next, the tangential components of the electromagnetic field at the surface of an integrated circuit (that couple to and excite the microcircuits) are derived for an incident electromagnetic wave or pulse. These fields as well as reflected and transmitted wave power depend in detail on the complex reflection coefficient which also is given in both exact and approximate forms. Then, the effects of signal path electrical parameters in crosstalk and coupling is investigated and the coupled responses (or cross impulse and step responses) are determined in analytical form based on a circuit-theoretic model. Finally, the three-layer geometry of an integrated circuit excited by an infinitesimal oscillating current moment at the substrate surface is analyzed to determine approximate analytical expressions for the complete electromagnetic field at other points on the surface. Aside from the quasistatic near fields, further coupling and interference can occur due to the radiation of both a surface wave in the substrate and a lateral wave above the substrate.

2. Summary of Research Results

Each of the following six major research results is discussed in more detail in a separate section of this report.

- Complete analytical expressions for propagating waves of voltage, current, and power in the time domain for three different transmission-line models of integrated circuit signal paths.
- Determination of finite-energy and finite-power voltage pulse shapes that are matched to the signal path and/or load to produce maximum current and instantaneous power.
- Development of the concept of the nominal resistance of a complex impedance which can be used to predict maximum possible path/load currents.
- Derivation of the complex reflection coefficient and tangential electromagnetic fields at the surface of an integrated circuit due to an incident electromagnetic wave or pulse.
- Analysis of inductive and capacitive coupling mechanisms in integrated circuits to determine coupled or cross-impulse and cross step responses and their dependence on lumped parameters of the signal paths.
- Theoretical study of the complete electromagnetic field produced by an infinitesimal oscillating current moment located on the dielectric substrate of an integrated circuit including discovery of a propagating surface wave (in the substrate) and a lateral wave (above the substrate).

Technical Papers:

"Nominal Resistance of a Complex Impedance," Electronics Letters, vol. 22, no. 13, pp. 703-704, June 1986.

"Peak Transient Current and Power into a Complex Impedance: Theory and Experiment," (in review), 31 pages, 12 figures, 1 table, May 1986.

"Cross Impulse and Step Response Models for Capacitive and Inductive Coupling in Very-High-Speed Integrated Circuits," (in preparation), June 1986.

"The Propagation of Signals Along a Three-Layered Region," (in preparation), August 1986.

Scientific Personnel:

D. Preis, Ph.D. (Principal Investigator)
Associate Professor of Electrical Engineering
Tufts University, Medford, MA 02155

R. W. P. King, Ph.D. (Consultant)
Professor of Applied Physics (Emeritus)
Harvard University, Cambridge, MA 02138

3. Distributed-Circuit Signal Path Characteristics

In an integrated circuit signal path the circuit parameters (resistance, capacitance, inductance, and conductance) are distributed on a per-unit-length basis. Therefore, conventional circuit analysis, which concentrates or "lumps" these parameters into circuit elements, is not an accurate approximation unless the frequency of operation is very low. If the actual waveshape of the voltage or current that propagates along the path is required then a distributed circuit (or transmission-line) model of the signal path is a better approximation.

The purpose of this section is to present analytical formulas derived for voltage, current, and power (energy/time) as a function of time and position on the signal path for three different distributed circuit models. The response of these different models to a unit step of input voltage is given. Path response to an arbitrary logic sequence of voltage step transitions can be computed by superposing step responses.

Figure 3.1 is a schematic representation of an integrated circuit signal path excited at time t = 0 by a unit step function of voltage (a transition at t = 0 from zero to one volt). The problem is to find the path voltage v(x, t) and current i(x, t) at a distance x from the source when the distributed parameters R, C, G, and L, the series resistance, shunt capacitance, shunt conductance, and series inductance (all per unit length) are specified.

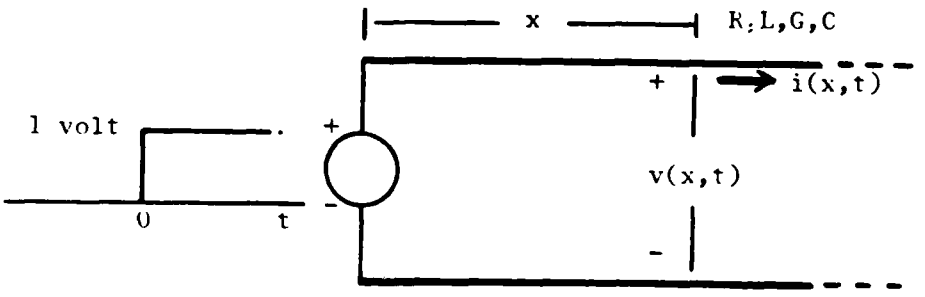

Fig. 3.1 Voltage and current at position x on signal path due to input voltage step.

Case 1. G = L = 0. Here it is assumed that series inductance and shunt conductance are negligible. (In an integrated-circuit signal path model these parameters are very small.) This is called the RC line or Thomson cable. The voltage v(x, t) in response to a unit step voltage input is,

$$v(x, t) = \text{erfc}\sqrt{\frac{x^2RC}{4t}} \text{ volts,} \tag{3.1}$$

where erfc(y) is the complementary error function of y. Rational function approximations of the error function and its complement are available in Handbook of Mathematical Functions (Abramowitz and Stegun, eds.) #7.1.27 and #7.1.28, page 299. The current that flows in response to a unit step voltage input is,

$$i(x, t) = \sqrt{\frac{C}{\pi Rt}}\, e^{-x^2RC/(4t)} \text{ amp.} \tag{3.2}$$

In (3.1) and (3.2) the quantity x^2RC is the product of total path resistance and capacitance of the path of length x. The voltage rises to 50% of its final value in approximately x^2RC seconds; the current maximum occurs at $t = 0.5\ x^2RC$ and, the instantaneous power (product of voltage and current) is a maximum when $t = 1.6\ x^2RC$. Thus the quantity x^2RC is like a time constant that gives an order-of-magnitude estimate of the "speed" of the RC line. Stated in different terms, "slowness" of the signal path is proportional to path length squared and the RC product.

Case 2. L = 0. If the shunt conductance G of the signal path is significant (due to losses in the dielectric substrate) then it is necessary to include a non-zero G in the analysis. This yields the so-called "leaky cable." There are two loss mechanisms, the resistance of the conducting signal path itself and the conductance of insulating substrate medium. The results of an analysis for the voltage and current in response to a unit step voltage input are,

$$v(x,\ t) = e^{-Gt/C}\left\{\operatorname{erfc}\sqrt{\frac{x^2RC}{4t}} + \frac{G}{C}\int_0^t \operatorname{erfc}\sqrt{\frac{x^2RC}{4\tau}}\ e^{-G\tau/C}\,d\tau\right\}, \quad (3.3)$$

and,

$$i(x,\ t) = e^{-Gt/C}\left\{\sqrt{\frac{C}{\pi Rt}}\ e^{-x^2RC/(4t)} + \int_0^t \sqrt{\frac{C}{\pi R\tau}}\ e^{-x^2RC/(4\tau)}e^{-G\tau/C}\,d\tau\right\}. \quad (3.4)$$

Comparison of (3.3) and (3.4) with (3.1) and (3.2) indicates that there are two effects of the "leakage" caused by shunt conductance G. First, the current and voltage waves are attenuated exponentially in time by the factor $e^{-Gt/C}$. Secondly, a component is added to each response consisting of a progressive integral of the attenuated wave. The major effect of G is attenuation of signal strength due to loss. A secondary effect is waveshape change of the step responses. Both of these effects can be minimized by reducing the G/C ratio or increasing path capacitance per unit length.

In both Cases 1 and 2 the absence of inductance L eliminates the usual propagation delay of $x\sqrt{LC}$ seconds normally associated with transmission lines. Each of the previous cases represents overdamped propagation because the ratio of attenuation constant to phase constant is equal to or greater than one so that waves damp out in less than one wavelength. Although they are more complicated, (3.3) and (3.4) are probably a better approximation to the physical situation and could be used, for example, to "fit" experimentally measured data.

There are two factors affecting overall "speed" of the signal path. The first is the slowness and attenuation of a step transition due to characteristic times associated with resistance/capacitance combinations (e.g., x^2RC and C/G seconds). The second factor is the introduction of an overall propagation delay equal to $x\sqrt{LC}$ seconds when series inductance $L \neq 0$. While the series inductance is normally very small, it does affect voltage and current waveshapes, too. These considerations lead to the third, and most general, case in which all parameters

R, C, G, and L are non-zero.

Case 3. All parameters non-zero. The voltage and current in response to a unit voltage step excitation of the general line is more complicated than in the previous two cases but still computationally tractable. Owing to a propagation delay of $x\sqrt{LC}$ seconds, both responses are zero until $t \geq x\sqrt{LC}$ when they have the general form,

$$v(x, t) = e^{-\frac{1}{2}\left(\frac{R}{L} + \frac{G}{C}\right)x\sqrt{LC}} \tag{3.5}$$

$$+ \left(\frac{R}{L} - \frac{G}{C}\right)x\sqrt{LC} \int_{x\sqrt{LC}}^{t} e^{-\frac{1}{2}\left(\frac{R}{L} + \frac{G}{C}\right)\tau} \cdot \frac{I_1\left[\frac{1}{2}\left(\frac{R}{L} - \frac{G}{C}\right)\sqrt{\tau^2 - x^2LC}\right]}{\sqrt{\tau^2 - x^2LC}} d\tau,$$

and,

$$i(x, t) = \sqrt{\frac{C}{L}} \left\{ e^{-\frac{1}{2}\left(\frac{R}{L} + \frac{G}{C}\right)t} I_o\left[\frac{1}{2}\left(\frac{R}{L} - \frac{G}{C}\right)\sqrt{t^2 - xLC}\right] \right. \tag{3.6}$$

$$\left. + \frac{G}{C} \int_{x\sqrt{LC}}^{t} e^{-\frac{1}{2}\left(\frac{R}{L} + \frac{G}{C}\right)\tau} I_o\left[\frac{1}{2}\left(\frac{R}{L} - \frac{G}{C}\right)\sqrt{\tau^2 - x^2LC}\right] d\tau \right\},$$

for $t \geq x\sqrt{LC}$. The modified Bessel functions of the first kind $I_o(y)$ and $I_1(y)$ in (3.5) and (3.6) are represented by rational approximations in Handbook of Mathematical Functions (Abramowitz and Stegun, Eds.) #9.8.1 through #9.8.4, page 378.

Two combinations of the four line parameters appear in (3.5) and (3.6). The combination (R/L + G/C) is an attenuation or damping term while the combination (R/L - G/C) is proportional to the amount of signal linear distortion the line causes (in the distortion-free line R/L = G/C, so that the distortion terms are zero).

In summary, (3.1) through (3.6) are complete analytical expressions for the voltage wave v(x, t) and current wave i(x, t) that propagate along a transmission-line signal path model when excited by a unit step function of voltage. The corresponding power flow p(x, t) is the product of these two waves and equals the energy/time at the position x and at time t. Equations (3.1) and (3.2), for the RC line, are valid when both the series inductance L and shunt conductance G of the path can be neglected. When substrate losses are significant, the shunt conductance G must be included. This leads to (3.3) and (3.4) in which the current and voltage waves of the RC line are attenuated and distorted due to the G/C ratio. If finite series inductance is incorporated then an overall propagation delay $x\sqrt{LC}$ seconds is introduced and both the voltage and current waves consist of distorted and non-distorted parts. These last results are more complicated because they involve integrals of Bessel functions.

The three different transmission-line or distributed circuit models of integrated circuit signal paths presented here are useful because they give the voltage and current waves in the time-domain (which can be compared directly to experimental measurements). Using these models the engineering tradeoffs between pulse strength, shape, propagation characteristics and ohmic losses can be computed for arbitrary choices of path parameters.

In practice, the actual signal path is finite and terminated with some load. This gives rise to reflected waves of voltage and current. These can be computed knowing the incident wave and load.

A more rigorous and comprehensive analytical approach to this general problem would use a field-theoretic analysis to determine all possible modes of wave propagation including a determination of the complex wavenumber k_c for the current that propagates along the conducting signal path. An analysis of this sort would reveal the extent to which distributed-circuit transmission-line models accurately represent dominant wave phenomena on integrated circuit signal paths. An alternative approach is to compare predictions from transmission-line models with experimental measurements on actual signal paths.

4. Nominal Resistance and Matching

Two important issues to consider when devising an optimum signal pulse launch-propagate-receive system are: (1) how to match a voltage pulse shape to the input impedance of the loaded signal path or to the load itself in order to maximize the input current and power, and (2) given the voltage pulse shape, how is the optimum signal path or load impedance determined. Two classes of voltage signals were considered. First, where the total energy of the input voltage is fixed and its shape is to be determined. Second, where the maximum amplitude of the voltage signal is limited and its transitions from maximum to minimum value are to be determined. A secondary consideration is whether operation is bandlimited. Both of these problems have been solved and simple formulas for the voltage signals and their relation to load impedance are available.

For each class of input signal (i.e., finite energy or finite power) a new quantity called the nominal resistance of a complex impedance was defined as the ratio of peak applied voltage to peak current under matched conditions. Nominal resistance is a function of the electrical properties of the signal path and/or load, namely, the inverse Fourier transform of the reciprocal of the impedance. Thus, knowing the nominal resistance and the class of input voltage signal the maximum (or peak) path or load current can be predicted.

A summary of the mathematical details and some supporting experimental data are included in the reprint (see next page) "Nominal Resistance of a Complex Impedance," Electronics Letters, vol. 22, no. 13, pp. 703-704, June 1986. A more comprehensive paper on this general subject entitled, "Peak Transient Current and Power into a Complex Impedance: Theory and Experiment" (31 pages, 12 figures, 1 table) is currently in review.

NOMINAL RESISTANCE OF A COMPLEX IMPEDANCE

Indexing terms: Circuit theory and design, Time-domain analysis, Impedance

The theoretical relationships between broadband electrical input impedance and maximum instantaneous input current are given for classes of input voltage signals with or without bandwidth limitations. A nominal resistance associated with a complex impedance is defined, and this quantity can be used in circuit analysis or design to predict maximum possible transient current. Results from several experimental measurements are presented.

When a complex load impedance $Z(\omega)$ is driven by an arbitrary voltage waveform $v(t)$, the maximum value i_{max} of the transient current $i(t)$ that flows into the load cannot be predicted without carrying out a detailed mathematical analysis to obtain the transient response in analytical form.[1] This is impractical when $v(t)$ is a member of a class of unpredictable waveforms such as, for example, a logic sequence of step transitions, a noise process or finite-energy analogue signals corresponding to segments of speech or music. Prior knowledge of i_{max} is essential, however, when specifying the output current and power capabilities of the circuit that produces the voltage $v(t)$ to drive the load impedance $Z(\omega)$. Three specific, practical examples are (i) estimating interstage peak currents in amplifiers, (ii) predicting logic-line-driver peak currents in integrated circuits, and (iii) determining audio-power-amplifier peak output current required to drive a given loudspeaker system.

In this letter a new quantity is introduced, called the nominal resistance associated with $Z(\omega)$, defined as the ratio of peak applied voltage to peak current. Nominal resistance depends not only on $Z(\omega)$ but also on the class of input signal (finite energy or finite power) and the operating bandwidth. Knowing the nominal resistance, the maximum possible peak current can be predicted for design or analysis purposes.

The current $i(t)$ that flows into a complex impedance $Z(\omega)$ in response to a voltage $v(t)$ is given by the temporal convolution

$$i(t) = \int_{-\infty}^{\infty} v(x)y(t-x)\,dx \tag{1}$$

where

$$y(t) = \frac{1}{2\pi}\int_{-\infty}^{\infty} Y(\omega)e^{j\omega t}\,d\omega \tag{2}$$

which is the inverse Fourier transform of the admittance $Y(\omega) = 1/Z(\omega)$. The quantity $y(t)$ can also be interpreted as the current in response to a unit impulse of voltage.

Two separate problems are considered here. First, maximise the current $i(t)$ when the total energy E of $v(t)$ is finite:

$$0 < E = \int_{-\infty}^{\infty} v^2(t)\,dt < \infty \tag{3}$$

that is, find the shape of $v(t)$. Secondly, maximise $i(t)$ when the amplitude of $v(t)$ is restricted by

$$0 < |v(t)| \le v_0 < \infty \tag{4}$$

where v_0 is a constant. It is assumed that eqn. 2 exists and that if $y(t)$ contains singularity functions they are of order no higher than a delta function $\delta(t)$. Thus, for example, $Z(\omega)$ may not contain a capacitor across its input terminals.

The solution to the first problem, from the matched-filter principle,[2] is

$$v_m(t) = k y(-t) \tag{5}$$

where the constant k is determined from eqn. 3. The peak current squared, in response to eqn. 5, is[2]

$$i_m^2(0) = E\int_{-\infty}^{\infty} y^2(t)\,dt = \frac{E}{2\pi}\int_{-\infty}^{\infty} |Y(\omega)|^2\,d\omega \tag{6}$$

with E specified by eqn. 3. The ratio of peak voltage to peak current or nominal resistance for the matched-filter input voltage eqn. 5, found from combining eqns. 3, 5 and 6, is

$$R_m = \frac{\max\,[y(t)]}{\int_{-\infty}^{\infty} y^2(t)\,dt} \tag{7}$$

For the second problem, the convolution eqn. 1 is maximised when the input voltage is

$$v_n(t) = v_0\ \text{sign}\,[y(-t)] \tag{8}$$

The peak current in response to eqn. 8 is

$$i_n(0) = v_0\int_{-\infty}^{\infty} |y(t)|\,dt \tag{9}$$

The nominal resistance, corresponding to eqns. 8 and 9, is

$$R_n = \frac{1}{\int_{-\infty}^{\infty} |y(t)|\,dt} \tag{10}$$

If operation is limited to the finite bandwidth σ rad s, then substitution of $y_\sigma(t)$ for $y(t)$ in eqns. 7 and 10 is necessary, where $y_\sigma(t)$ is computed from eqn. 2 using finite integration limits $\pm\sigma$.

Fig. 1 illustrates impedance magnitude against frequency for a 14·35 Ω carbon resistor R and five different complex impedances numbered 1–5. These data were measured digitally and represent discrete values every 48 Hz throughout a 20 kHz bandwidth. Table 1 lists both the DC value ($\omega = 0$) and minimum value (for $\omega > 0$) of the impedance magnitudes in Fig. 1. The quantity $y(t)$ in eqn. 2 was estimated for each

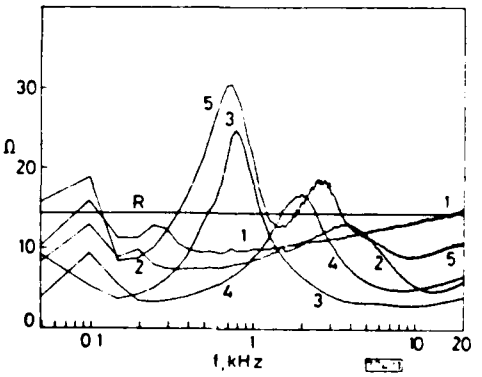

Fig. 1 *Input impedance magnitude of 14·35 Ω resistor R and five different complex impedances*

impedance as the current in response to a 20 μs-wide rectangular voltage pulse. Using 1024 samples (50 kHz sampling frequency) of each $y(t)$, based on an average of 2000 trials to improve signal/noise ratio, nominal resistances were evaluated numerically by approximating the integrals in eqns. 7 and 10 with finite sums. The resulting numerical values of R_n and R_m are also given in Table 1.

Examination of the data in Table 1 will reveal that R_m, the nominal resistance corresponding to a matched-filtered, finite-energy input voltage, was not found to be less than the minimum impedance magnitude, but R_n, the nominal resistance for a voltage-limited finite-power input, can be approximately half of the minimum impedance magnitude.

The accuracy of a nominal resistance computation depends on how well the quantity $y(t)$ in eqn. 2 is estimated experimen-

Table 1

Impedance	$Z(0) = R_{DC}$	$\lvert Z(\omega)\rvert_{\min}$ $\omega > 0$	R_m	R_n
	Ω	Ω	Ω	Ω
R	14·35	14·35	14·35	14·35
1	8·84	9·38	10·86	6·12
2	6·18	4·67	6·89	3·12
3	7·05	2·95	3·84	1·51
4	3·57	3·28	6·18	1·86
5	20·66	8·38	11·97	4·67

tally. Comparison of the inverse FFT of the sampled values of $y(t)$ derived from the 20 μs pulse measurements indicated that the admittance spectral magnitude $|Y(\omega)|$ was within ± 1 dB of the true admittance magnitude measured independently. In this connection, it also is possible to estimate $y(t)$ using different voltage pulse shapes or, indirectly, as the inverse FFT of the measured complex admittance.

D. PREIS*

Department of Electrical Engineering
Tufts University
Medford, MA 02155, USA

6th May 1986

References

1 PREIS, D.: 'A catalog of frequency and transient responses', *J. Audio Eng. Soc.*, 1977, **25**, pp. 990–1007

2 PAPOULIS, A.: 'Maximum response with input energy constraints and the matched-filter principle', *IEEE Trans.*, 1970, **CT-17**, pp. 175–182

Reprinted from ELECTRONICS LETTERS 19th June 1986 Vol. 22 No. 13 pp. 703-704

5. Peak Path Currents and Interference

The concept of nominal resistance introduced in the previous section has further application in the study of crosstalk, inductive coupling, and interference between signal paths. For a given signal path and/or load there exists a specific logic sequence that will excite extremely large peak instantaneous currents (as well as large rates of change of current). Such currents can potentially interfere with other circuits through the mechanism of inductive coupling. If the input impedance of the path and/or load is $Z(\omega)$ then the logic sequence producing the maximum possible value of instantaneous current is produced by the voltage $v(t) = v_o \text{sign}[y(-t)]$ where v_o is the maximum voltage of the logic sequence and $y(t)$ is the inverse Fourier transform of $Y(\omega) = 1/Z(\omega)$. The peak current and nominal resistance formula are given in equations (9) and (10), respectively, of the reprint in the previous section.

When, in analysis or design of integrated circuit signal paths and loads, the question of maximum possible instantaneous current arises, the answer is simple and direct. The maximum possible transient current i_{max} in response to any logic sequence is given by a formula similar in form to Ohm's Law, namely, $i_{max} = v_o/R_n$. In this equation, R_n is the nominal resistance of the path and v_o the maximum voltage of the logic sequence. Thus nominal resistance is an important new parameter that characterizes a signal path and/or load. The smaller R_n is the larger the maximum transient current can be. Nominal resistance can be calculated from $y(t)$, the current in response to a unit impulse excitation of the signal path, using equation (10) in the previous section. The currents $i(x, t)$ in (3.2), (3.4), and (3.6) of section 3 of this report can be used to compute R_n for transmission line models of signal paths if they are first differentiated with respect to time (because they are the currents in response to a unit step rather than impulse of voltage).

6. Incident Electromagnetic Waves or Pulses

In terms of high-frequency electromagnetic fields an integrated circuit is a three-layer problem consisting of air above, a lossy dielectric substrate, and an imperfectly conducting metal ground plane underneath. When this circuit is illuminated from above by an incident electromagnetic plane wave (or an electromagnetic pulse consisting of a superposition of plane waves of different frequencies) part of each wave is reflected away and the remainder transmitted (refracted) into the dielectric substrate and conducting layers.

An important quantity, which completely characterizes the reflection of incident electromagnetic waves at the air-dielectric interface, is the complex reflection coefficient f_r. The squared magnitude of the reflection coefficient $0 \leq |f_r|^2 \leq 1$ is a direct measure of the ratio of reflected power to incident power. The reflection coefficient f_r depends on the electromagnetic properties of each of the three layers (i.e., permittivity, permeability, and conductivity), the incident wave's frequency, and the orientation of the incident wave's electric and magnetic vectors with respect to the plane of incidence.

For a given three-layer geometry, $|f_r|^2$ indicates what proportion of the incident wave's power is reflected (harmlessly) away while (potentially damaging) wave power that is absorbed by the integrated circuit is $1 - |f_r|^2$. Therefore, to minimize possible damage to an integrated circuit caused by an incident electromagnetic wave of frequency ω, the reflection coefficient at that frequency should be $|f_r| \sim 1$ for all likely angles of incidence. When dealing with an incident, high-energy electromagnetic pulse, the potentially damaging effects of electromagnetic radiation are minimized when $|f_r| \sim 1$ for those frequency ranges throughout which the spectrum of the pulse contains significant energy.

The reflection coefficient also provides insight into the problem of shielding or radiation hardening of integrated circuits. Because the three-layer geometry and its electromagnetic properties as well as the frequency range of incoming electromagnetic energy (usually) are all given quantities, the frequency ranges where the reflection coefficient

$|f_r| \sim 0$, or small compared with unity are vulnerable and, consequently, do need some external shielding.

The fact that f_r is a complex function (i.e., having both magnitude and phase) has further technical implications. Certain incident pulse shapes may produce extremely high momentary field strengths in the integrated circuit if they are, for example, conjugate matched to the complex transmission coefficient (which is related to the reflection coefficient). This situation is similar to matched filtering. Due to phase linearization, waves superpose at one instant in time rather than being dispersed in time. Thus, information provided by the complex transmission coefficient is useful in two ways. First, to shield against such pulses and, secondly, to design electromagnetic pulse shapes that are, for a given energy, potentially most damaging to integrated circuits.

A further use of the complex reflection coefficient is in the determination of the tangential components of the electric and magnetic field at the interface between air and dielectric surface. These fields can excite (couple to) the circuits on the dielectric surface.

Figure 6.1 shows the three-layer geometry consisting of air (Region 0), dielectric (Region 1), and conductor (Region 2). Consider a

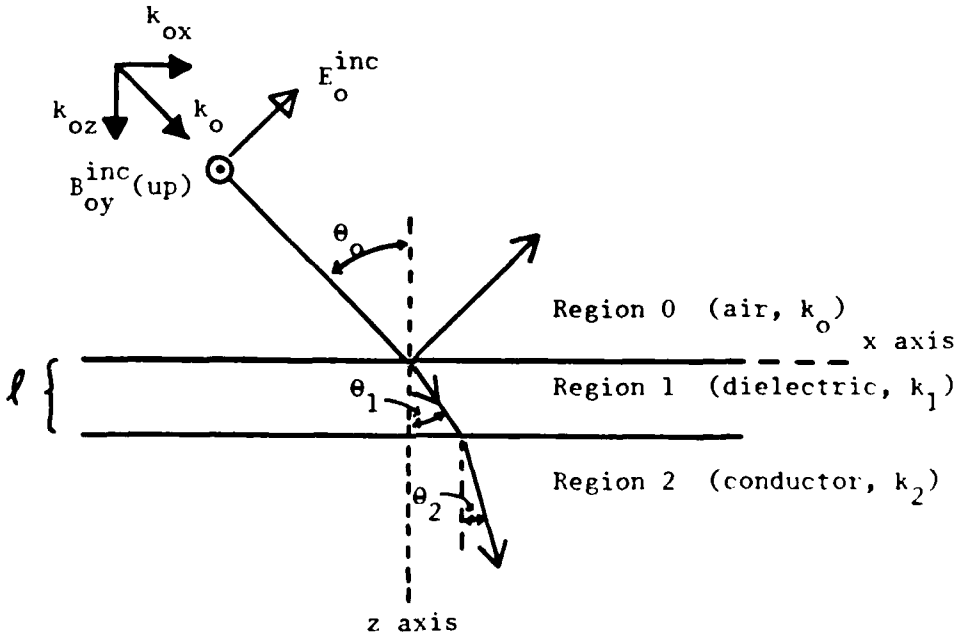

Fig. 6.1 Plane wave incident on boundary $z = 0$ of dielectric Region 1.

plane wave incident from the air (Region 0, $z \leq 0$) on the plane boundary $z = 0$ between regions 0 and 1 as shown in Fig. 6.1. Region 1 has uniform thickness ℓ and is bounded at $z = \ell$ by Region 2 ($z \geq \ell$).

The complex wave number in each region is,

$$k_j = \beta_j + i\alpha_j = \omega[\mu_o(\epsilon_j + i\sigma_j/\omega)]^{1/2}, \quad j = 0, 1, 2, \tag{6.1}$$

where ϵ and σ are the real, effective permittivity and conductivity, respectively, and the permeability μ_o is, by assumption, that of air. The angles θ_o, θ_1, and θ_2 in Fig. 6.1 are related by Snell's law.

For an electromagnetic field of the electric type (i.e., with the electric field in the plane of incidence), the result of a lengthy derivation for the complex reflection coefficient f_{er} is,

$$f_{er} = \frac{k_2\cos\theta_o - k_o\cos\theta_2 - i\left[\dfrac{k_1\cos\theta_2\cos\theta_o}{\cos\theta_1} - \dfrac{k_o k_2\cos\theta_1}{k_1}\right]\tan(k_1\ell\cos\theta_1)}{k_2\cos\theta_o + k_o\cos\theta_2 - i\left[\dfrac{k_1\cos\theta_2\cos\theta_o}{\cos\theta_1} + \dfrac{k_o k_2\cos\theta_1}{k_1}\right]\tan(k_1\ell\cos\theta_1)}. \tag{6.2}$$

With the notation,

$$\vec{k} = \hat{x}k_x + \hat{z}k_z, \quad k_x = k\sin\theta \text{ and } k_z = k\cos\theta, \tag{6.3}$$

the reflection coefficient can be expressed as,

$$f_{er} = \frac{k_2^2 k_{oz} - k_o^2 k_{2z} - i\left[k_1^2 k_{oz}\left(\dfrac{k_{2z}}{k_{1z}}\right) - k_o^2 k_{1z}\left(\dfrac{k_2^2}{k_1^2}\right)\right]\tan(k_{1z}\ell)}{k_2^2 k_{oz} + k_o k_{2z} - i\left[k_1^2 k_{oz}\left(\dfrac{k_{2z}}{k_{1z}}\right) - k_o^2 k_{1z}\left(\dfrac{k_2^2}{k_1^2}\right)\right]\tan(k_{1z}\ell)}. \tag{6.4}$$

This is the general formula for the plane-wave reflection coefficient of the electric type for the three-layered region.

The general formula (6.4) can be simplified with the practically valued inequalities,

$$\left|k_2^2\right| >> \left|k_1^2\right| >> \left|k_o^2\right|, \left|\frac{k_1^2}{k_2^2}\right| << \left|\frac{k_o^2}{k_1^2}\right|, \left|k_{1z}\ell\right| \leq 1, \tag{6.5}$$

to the form,

$$f_{er} \cong \frac{k_2^2 k_{oz} - k_o^2 k_{2z}}{k_2^2 k_{oz} + k_o^2 k_{2z}} + 2i\ell\left(\frac{k_o^2 k_{1z}^2}{k_1^2 k_{oz}}\right). \tag{6.6}$$

In this approximation the first term is the reflection coefficient of the two-layered region with $\ell = 0$.

The electromagnetic field of electric type on the air-surface of the dielectric is,

$$B_{oy}(x, 0) = B_{oy}^{inc}(0,0)e^{ik_{ox}x}[1 + f_{er}], \tag{6.7}$$

$$E_{ox}(x, 0) = \frac{\omega}{k_o} B_{oy}^{inc}(0, 0)e^{ik_{ox}x}[1 - f_{er}]\cos\theta_o, \tag{6.8}$$

$$E_{oz}(x, 0) = \frac{-\omega}{k_o} B_{oy}^{inc}(0, 0)e^{ik_{ox}x}[1 - f_{er}]\sin\theta_o, \tag{6.9}$$

where f_{er} is given by (6.4) or (6.6). The tangential components $B_{oy}(x, 0)$ and $E_{ox}(x, 0)$ are of primary interest in the excitation of circuits on the dielectric surface.

The reflection coefficient for fields of the magnetic type (i.e., with the magnetic field in the plane of incidence) for the three-layer problem of Fig. 6.1 is,

$$f_{mr} = \frac{k_o\cos\theta_o - k_2\cos\theta_2 - \left[\frac{k_2\cos\theta_2 k_o\cos\theta_1}{k_1\cos\theta_1} - k_1\cos\theta_1\right]\tan(k_1\ell\cos\theta_1)}{k_o\cos\theta_o + k_2\cos\theta_2 - \left[\frac{k_2\cos\theta_2 k_o\cos\theta_o}{k_1\cos\theta_1} + k_1\cos\theta_1\right]\tan(k_1\ell\cos\theta_1)}. \tag{6.10}$$

With the notation,

$$k_x = k\sin\theta,\ k_z = k\cos\theta, \tag{6.11}$$

(6.10) becomes,

$$f_{mr} = \frac{k_{oz} - k_{2z} - i\left[\dfrac{k_{2z}-k_{oz}}{k_{1z}} - k_{1z}\right]\tan(k_{1z}\ell)}{k_{oz} + k_{2z} - i\left[\dfrac{k_{2z}k_{oz}}{k_{1z}} + k_{1z}\right]\tan(k_{1z}\ell)}. \tag{6.12}$$

This is the general form for the plane-wave reflection coefficient of the magnetic type for the three-layered region.

With the condition,

$$|k_{1z}\ell| \leq 1, \tag{6.13}$$

(6.12) simplifies to the form,

$$f_{mr} = \frac{k_{oz} - k_{2z}}{k_{oz} + k_{2z}} - 2ik_{oz}\ell. \tag{6.14}$$

In this approximation the first term is the reflection coefficient of the two-layer region obtained with $\ell = 0$.

The electromagnetic field of the magnetic type on the surface of the dielectric is,

$$E_{oy}(x, 0) = E_{oy}^{inc}(0, 0)e^{ik_{ox}x}[1 + f_{mr}], \tag{6.15}$$

$$B_{ox}(x, 0) = -\frac{k_o}{\omega} E_{oy}^{inc}(0, 0)e^{ik_{ox}x}[1 - f_{mr}]\cos\theta_o, \tag{6.16}$$

$$B_{oz}(x, 0) = \frac{k_o}{\omega} E_{oy}^{inc}(0, 0)e^{ik_{ox}x}[1 + f_{mr}]\sin\theta_o. \tag{6.17}$$

The tangential components $E_{oy}(x, 0)$ and $B_{ox}(x, 0)$ play an important role in exciting the electrical circuits on the dielectric surface.

In summary, the following new research results are contained in this section. For a plane wave of arbitrary angle of incidence on the dielectric surface of a three-layer model for an integrated circuit, the complex reflection coefficient is given in both exact and approximate analytical form for the electric field of the wave in the plane of incidence [(6.4) and (6.6)] and for the magnetic field of the wave in the plane of incidence [(6.12) and (6.14)]. The tangential components of the electromagnetic field capable of exciting circuits at the air-dielectric interface are given in exact analytical form [(6.7), (6.8), (6.9) and (6.15), (6.16), (6.17)]. These expressions are relatively simple and suitable for numerical computation. Because frequency ω is an arbitrary parameter contained in the complex wavenumbers (6.1), these results also are applicable to electromagnetic pulses composed of a superposition of (or spectrum of) plane waves. The general formulas can be used to analyze both existing geometries and materials or proposed new ones.

7. Circuit-Theoretic Path Coupling Model

The objective of this section is to present analytical formulas and curves for coupling between signal paths in integrated circuits based on lumped-parameter circuit theory models. While this is an oversimplification of the general coupling problem, the conclusions based on the analysis are consistent with those drawn from the more complicated field-theoretic path coupling model in section 8 of this report.

Simple, capacitively coupled RC circuits are analyzed to illustrate the time-domain and frequency-domain nature of capacitive coupling. Next, a more general coupled circuit, that includes both inductance and resistive loading of the signal path, is analyzed to show the effects of capacitive and inductive coupling separately. Analytical expressions are given for coupling gain and coupled (or cross) impulse and step responses. Several curves of cross impulse and step responses are presented. Means of reducing coupling are discussed.

Consider the elementary circuit in Fig. 7.1 used to model first-order capacitive coupling between signal paths on an integrated circuit. The lower RC line is driven by voltage $v_{in}(t)$ and coupled via the mutual capacitance C_m to the upper RC line which is not driven but has an output voltage $v_m(t)$ due to mutual coupling. The problem is to determine the voltage transfer function between v_{in} and v_m in the frequency domain, then find v_m when v_{in} is either an impulse or step function of voltage.

Assuming $C_m << C$, the current through C_m is small relative to that through C in the lower line and this leads to the voltage transfer function (in terms of the complex frequency variable s),

$$\frac{V_m(s)}{V_{in}(s)} \approx \frac{1}{1 + sRC} \left\{ \frac{sRC}{1 + sRC} \cdot \frac{C_m}{C} \right\}. \tag{7.1}$$

The term in front of the brackets is the voltage across C in the lower line while the term in the brackets represents the voltage coupled through C_m.

The magnitude of the spectrum of the transfer function (7.1) is shown

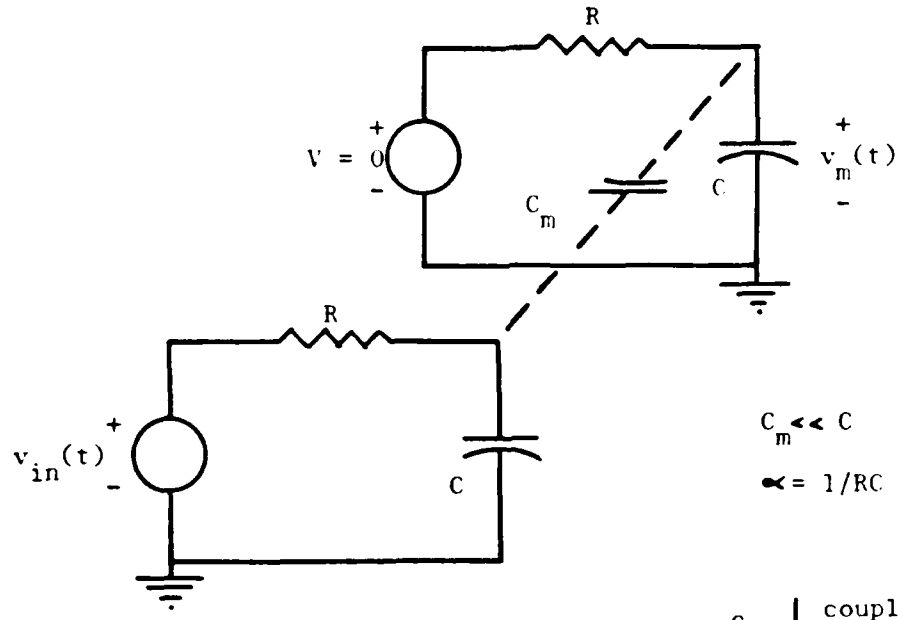

$C_m << C$

$\alpha = 1/RC$

$$\frac{V_m(s)}{V_{in}(s)} = \alpha \frac{s}{(s+\alpha)^2} \frac{C_m}{C}$$

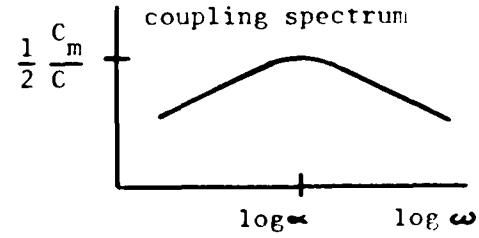

$$h(t) = e^{-\alpha t}(1 - \alpha t)\frac{C_m}{C}$$

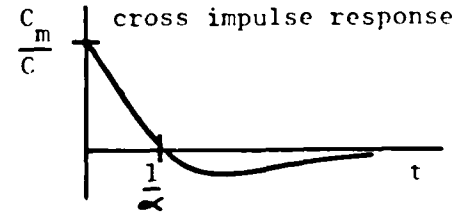

$$a(t) = \alpha t\, e^{-\alpha t} \frac{C_m}{C}$$

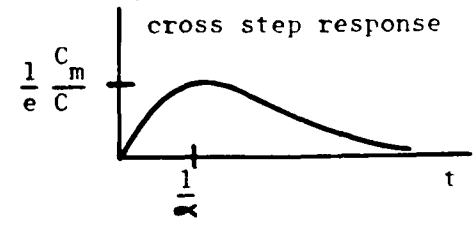

Fig. 7.1. First-order capacitive coupling: circuit, complex transfer function and coupling spectrum, coupled impulse response h(t), coupled step response a(t).

in Fig. 7.1. Coupling is bandpass having a maximum at the frequency $\omega = \alpha = 1/RC$ where the coupling coefficient equals $0.25\ C_m/C$. To either side of $\omega = \alpha$, coupling rolls off at 6dB/oct. The inverse transform of (7.1) yields the "cross-impulse response" h(t), that is, $h(t) = v_m(t)$ when $v_{in}(t) = \delta(t)$. When the lower line is excited by an impulse $\delta(t)$ the coupled voltage h(t) has the shape shown in Fig. 7.1. The peak value of h(t) equals $\alpha C_m/C$ and it occurs when t = 0. The areas under the positive and negative portions of the impulse response are equal and opposite. This occurs because the step response a(t), which equals the integral of h(t), has a final value of zero (corresponding to the zero-frequency value of the coupling transfer function). The maximum value of the step response is $0.368\ C_m/C$ and occurs at $t = 1/\alpha = RC$.

As Fig. 7.1 summarizes, the maximum of the voltage coupling coefficient, cross impulse and step responses are all proportional to C_m/C, the ratio of coupling capacitance to line capacitance. This ratio could be made small by increasing the capacitance of the signal path, or decreasing the mutual capacitance, or both.

A more realistic model would include some resistive loading at the end of each signal path as well as path inductance and inductive coupling. This increases both the order of the differential equations describing the circuits and the number of circuit parameters.

The objective of the second modelling approach to follow is to determine the voltage coupled from one signal path to another due to capacitive and inductive coupling. Each coupling mechanism is considered separately and both frequency-domain and time-domain responses are evaluated in analytical form. This lumped-parameter signal-path model provides considerably more insight into the nature of coupling. It quantitatively describes the dependence of coupled voltages on the parameters of the signal path, namely, path resistance, capacitance, inductance, loading and mutual capacitance and inductance.

Figure 7.2 shows the second lumped-parameter signal-path model. The lower and upper signal paths each have path resistance R, inductance L, and capacitance C and each path is loaded with a resistor R_o. Capacitive coupling between the two paths is taken into account by the

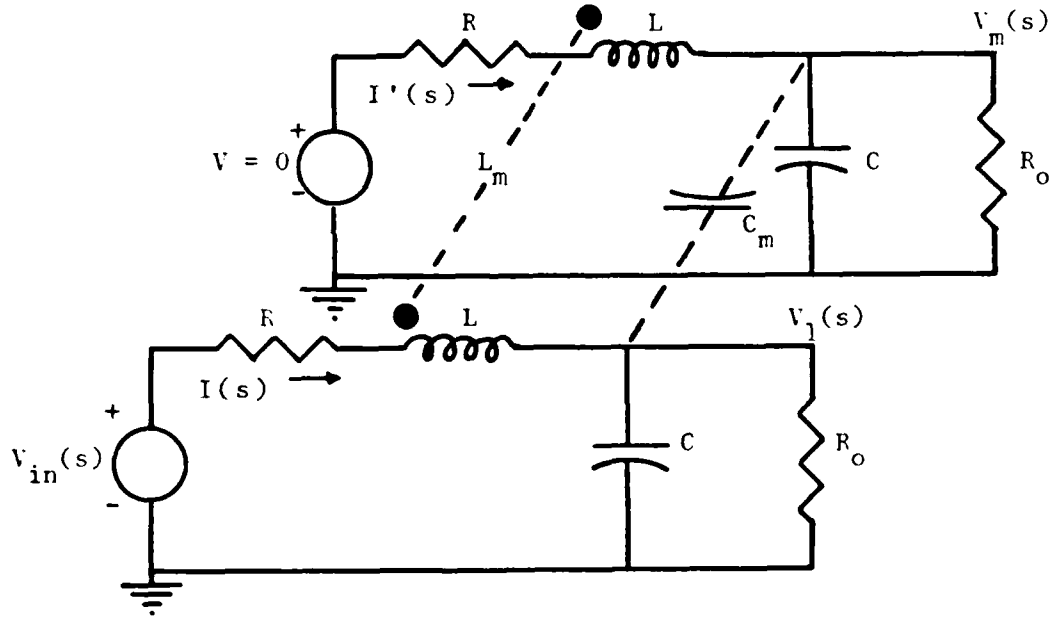

Fig. 7.2. Lumped-element model for capacitive and inductive coupling between signal paths used to evaluate cross impulse and cross step responses shown in Figs. 7.3-7.6.

mutual capacitance C_m and inductive coupling by mutual inductance L_m. Only five circuit parameters are needed to describe coupling: R, L, C, R_o, and C_m for capacitive coupling or R, L, C, R_o and L_m for inductive coupling. In Fig. 7.2, the lower signal path is excited with the arbitrary voltage $V_{in}(s)$, where $s = \sigma + j\omega$ is the complex frequency variable, and the voltage coupled to the (undriven) upper signal path is $V_m(s)$.

To denote <u>capacitive coupling</u> the notation $V_m(s) = V_m^C(s)$ is used. The voltage transfer function $V_m^C(s)/V_{in}(s)$ can be evaluated simply when it is assumed that the current through C_m is small compared to that through the parallel combination of C and R_o in the lower path. Also, the mutual inductance L_m is ignored. The result is,

$$\frac{V_m^C(s)}{V_{in}(s)} = \frac{C_m}{C} \cdot \frac{1}{LC} \cdot \frac{s(s + R/L)}{\left\{ s^2 + s\left(\frac{R}{L} + \frac{1}{R_o C}\right) + \frac{1}{LC}\left(1 + \frac{R}{R_o}\right)\right\}^2}. \tag{7.2}$$

The voltage transfer function is <u>bandpass</u> with maximum mid-frequency gain given by,

$$\frac{V_m^C(s)}{V_{in}(s)} \cong \frac{C_m}{C} \cdot \frac{1}{LC} \cdot \frac{1}{\left(\frac{R}{L} + \frac{1}{R_o C}\right)^2}. \tag{7.3}$$

At very high frequencies the gain rolls off at -12dB/octave and has the general form,

$$\frac{V_m^C(s)}{V_{in}(s)} \cong \frac{C_m}{C} \cdot \frac{1}{LC} \cdot \frac{1}{s^2}. \tag{7.4}$$

At low frequencies the gain rises at +6dB/octave and takes the form,

$$\frac{V_m^C(s)}{V_{in}(s)} = \frac{C_m}{C} \cdot \frac{sRC}{\left(1 + \frac{R}{R_o}\right)^2}. \tag{7.5}$$

These results show that, for fixed path parameters R, L, and C, capacitive coupling is reduced when either the mutual capacitance C_m and/or path load resistance R_o is decreased. When path parameters are adjustable, capacitive coupling is reduced by increasing the path capacitance C, keeping the mutual capacitance fixed, so that the ratio C_m/C decreases.

Transient responses can be derived from the general voltage transfer function (7.2) by inverse Laplace transformation. Two transient responses are of particular interest: the coupled voltage when the input is an impulse h(t) or unit step u(t). These coupled voltages (or cross impulse and step responses) are denoted by $h_m^C(t)$ and $a_m^C(t)$, respectively. When the cross impulse response is known the coupled response to an arbitrary input voltage waveform can be evaluated by temporal convolution. The cross step response yields the actual time-domain waveform of the coupled voltage due to a typical step transition of a logic sequence.

The impulse response $h_m^C(t)$ is the inverse Laplace transform of the voltage transfer function (7.2) which can be rewritten as,

$$\frac{V_m^C(s)}{V_{in}(s)} = \frac{C_m}{C} \cdot \frac{1}{LC} \cdot \frac{s(s + \alpha_3)}{(s + \alpha_1)^2 (s + \alpha_2)^2}, \tag{7.6}$$

where,

$$\alpha_1 = \frac{1}{2}\left(\frac{R}{L} + \frac{1}{R_o C}\right) + \frac{1}{2}\sqrt{\left(\frac{R}{L} + \frac{1}{R_o C}\right)^2 - \frac{4}{LC}\left(1 + \frac{R}{R_o}\right)}, \tag{7.7}$$

$$\alpha_2 = \frac{1}{2}\left(\frac{R}{L} + \frac{1}{R_o C}\right) - \frac{1}{2}\sqrt{\left(\frac{R}{L} + \frac{1}{R_o C}\right)^2 - \frac{4}{LC}\left(1 + \frac{R}{R_o}\right)}, \tag{7.8}$$

$$\alpha_3 = R/L. \tag{7.9}$$

There are three possibilities for the numerical values of the parameters α_1 and α_2: complex conjugates, real and equal, or real and distinct (depending on whether the quantity under the radical sign is negative, zero, or positive, respectively). Here, the last possibility is assumed, namely,

$$\left(\frac{R}{L} + \frac{1}{R_o C}\right)^2 > \frac{4}{LC}\left(1 + \frac{R}{R_o}\right). \tag{7.10}$$

Physically, this assumption implies that the coupling mechanism is overdamped so that the transient responses will consist of exponential terms of the form $e^{-\alpha t}$ or $te^{-\alpha t}$ rather than exponentially damped sinusoids.

When the voltage transfer function is expanded in a partial fraction expansion and its inverse Laplace transform taken, the cross impulse response is found to be,

$$h_m^C(t) = \frac{C_m}{C} \cdot \frac{1}{LC}\left\{(a_1 + b_1 t)e^{-\alpha_1 t} + (C_1 + d_1 t)e^{-\alpha_2 t}\right\}, \tag{7.11}$$

where the constants a_1 through d_1 are,

$$a_1 = \frac{\alpha_3(\alpha_1 + \alpha_2) - 2\alpha_1\alpha_2}{(\alpha_2 - \alpha_1)^3}, \tag{7.12}$$

$$b_1 = -\alpha_1 \frac{(\alpha_3 - \alpha_1)}{(\alpha_2 - \alpha_1)^2}, \tag{7.13}$$

$$C_1 = \frac{\alpha_3(\alpha_1 + \alpha_2) - 2\alpha_1\alpha_2}{(\alpha_1 - \alpha_2)^3}, \tag{7.14}$$

$$d_1 = -\alpha_2 \frac{(\alpha_3 - \alpha_2)}{(\alpha_1 - \alpha_2)^2}, \tag{7.15}$$

with α_1, α_2, and α_3 given in (7.7), (7.8), and (7.9), respectively.

Figures 7.3 and 7.4 are graphs of the cross impulse response (7.11) for several choices of parameters. The step response equals the integral with respect to time of the impulse response or the inverse Laplace transform of 1/s times the voltage transfer function (7.2). It is,

$$a_m{}^C(t) = \frac{C_m}{C} \cdot \frac{1}{LC}\left\{(a_2 + b_2 t)e^{-\alpha_1 t} + (c_2 + d_2 t)e^{-\alpha_2 t}\right\}, \tag{7.16}$$

where the constants a_2 through d_2 are,

$$a_2 = \frac{\alpha_1 + \alpha_2 - 2\alpha_3}{(\alpha_2 - \alpha_1)^3}, \tag{7.17}$$

$$b_2 = \frac{\alpha_3 - \alpha_1}{(\alpha_2 - \alpha_1)^2}, \tag{7.18}$$

$$c_2 = \frac{\alpha_1 + \alpha_2 - 2\alpha_3}{(\alpha_1 - \alpha_2)^3}, \tag{7.19}$$

$$d_2 = \frac{\alpha_3 - \alpha_2}{(\alpha_1 - \alpha_2)^2}, \tag{7.20}$$

with α_1, α_2, and α_3 given in (7.7), (7.8), and (7.9) respectively.

Figures 7.5 and 7.6 are graphs of the cross step response (7.16) for the same choices of parameters as in Figs. 7.3 and 7.4. In the denominator of every term of each transient response is the constant factor,

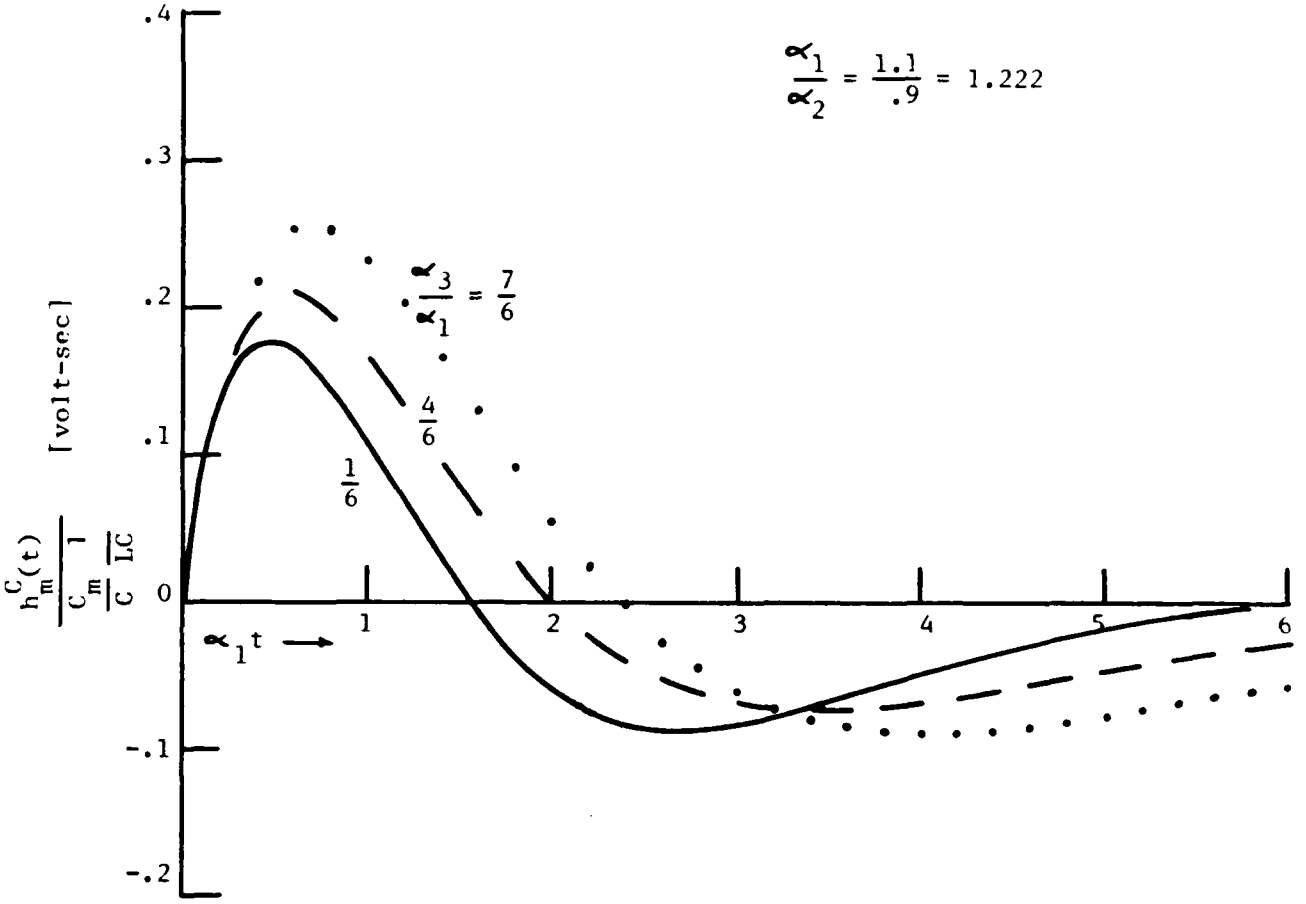

Fig. 7.3. Normalized capacitively coupled cross impulse responses vs. normalized time.

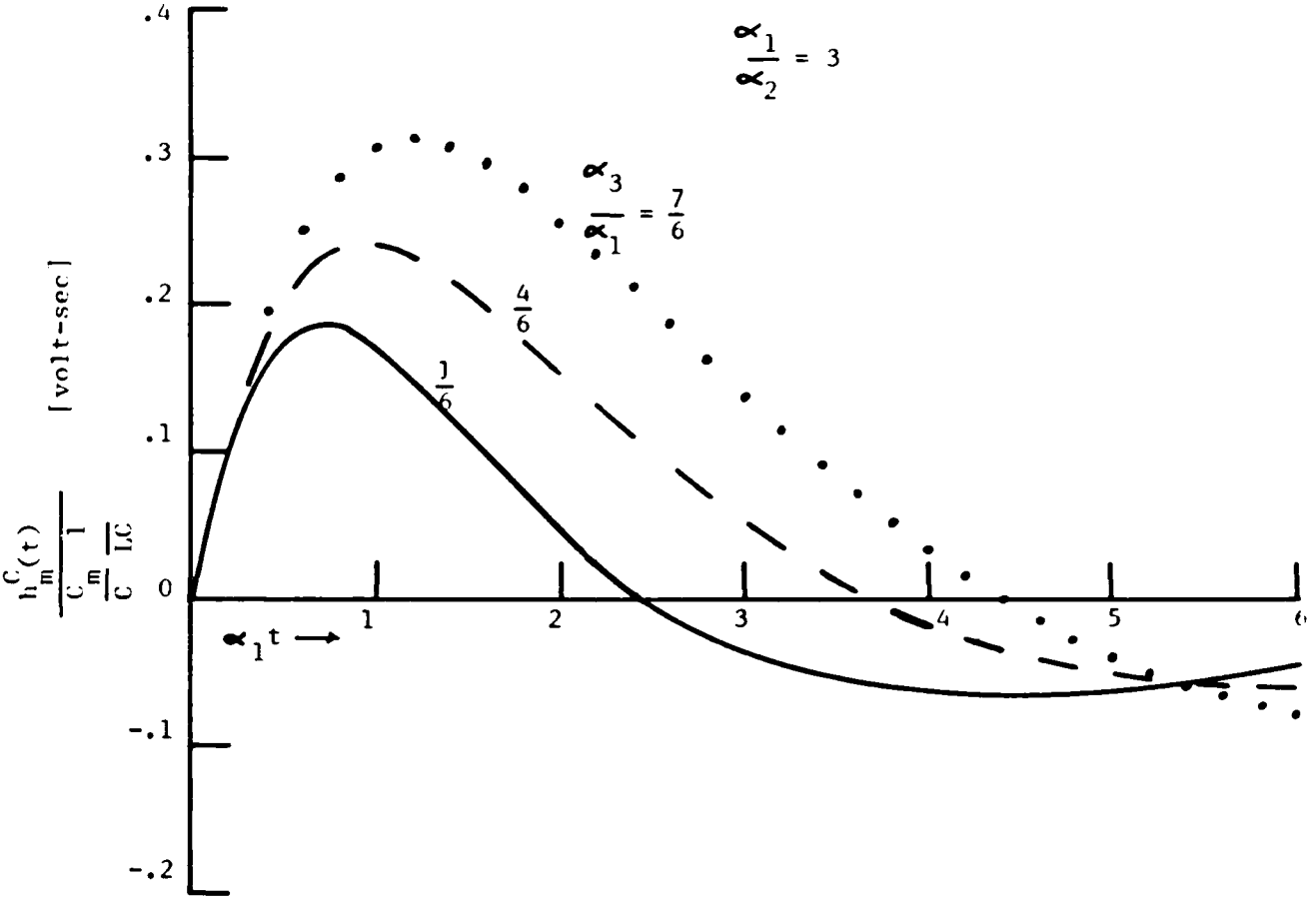

Fig. 7.4. Normalized capacitively coupled cross impulse responses vs. normalized time.

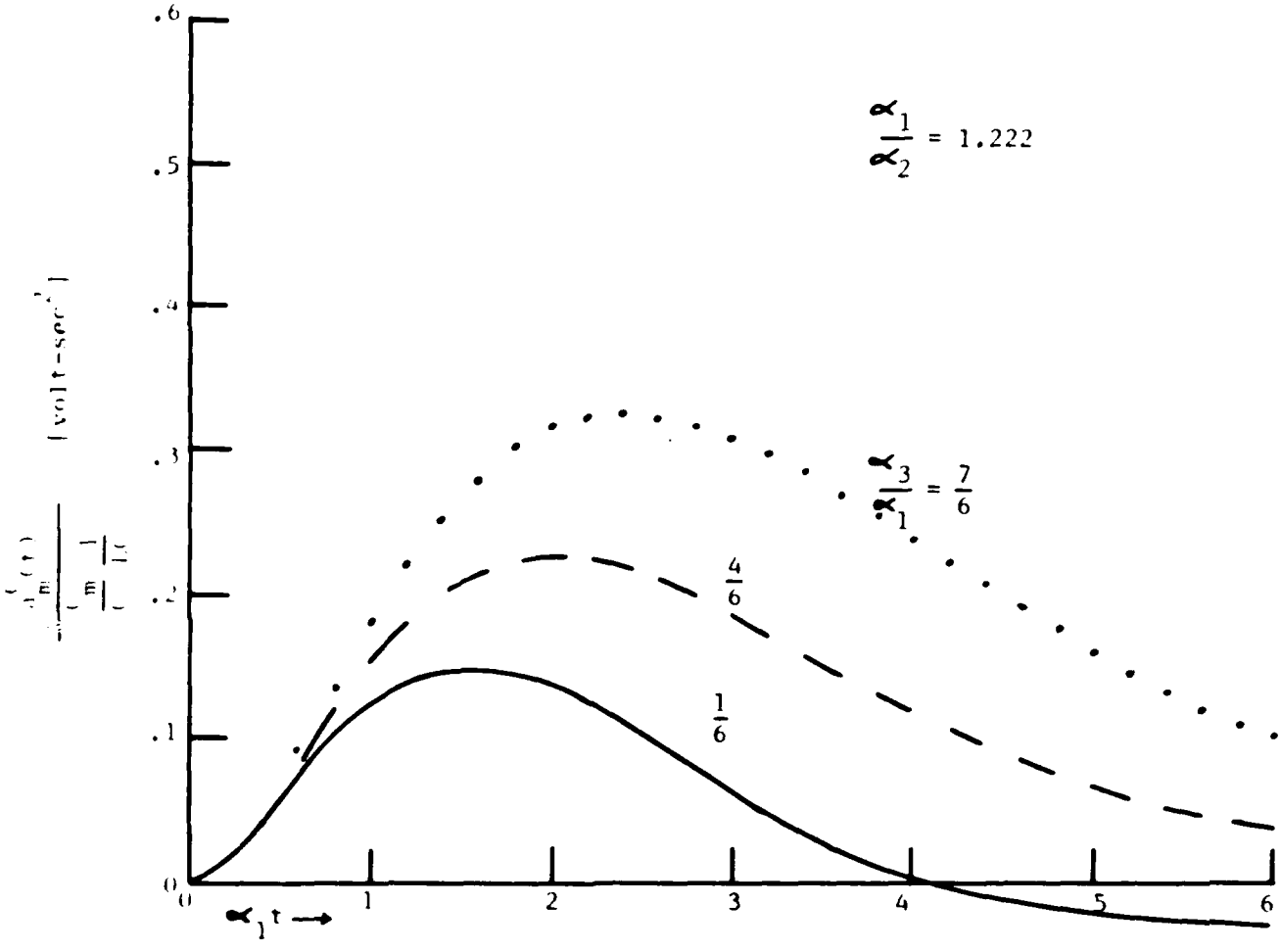

Fig. 7.5. Normalized capacitively coupled cross step responses vs. normalized time.

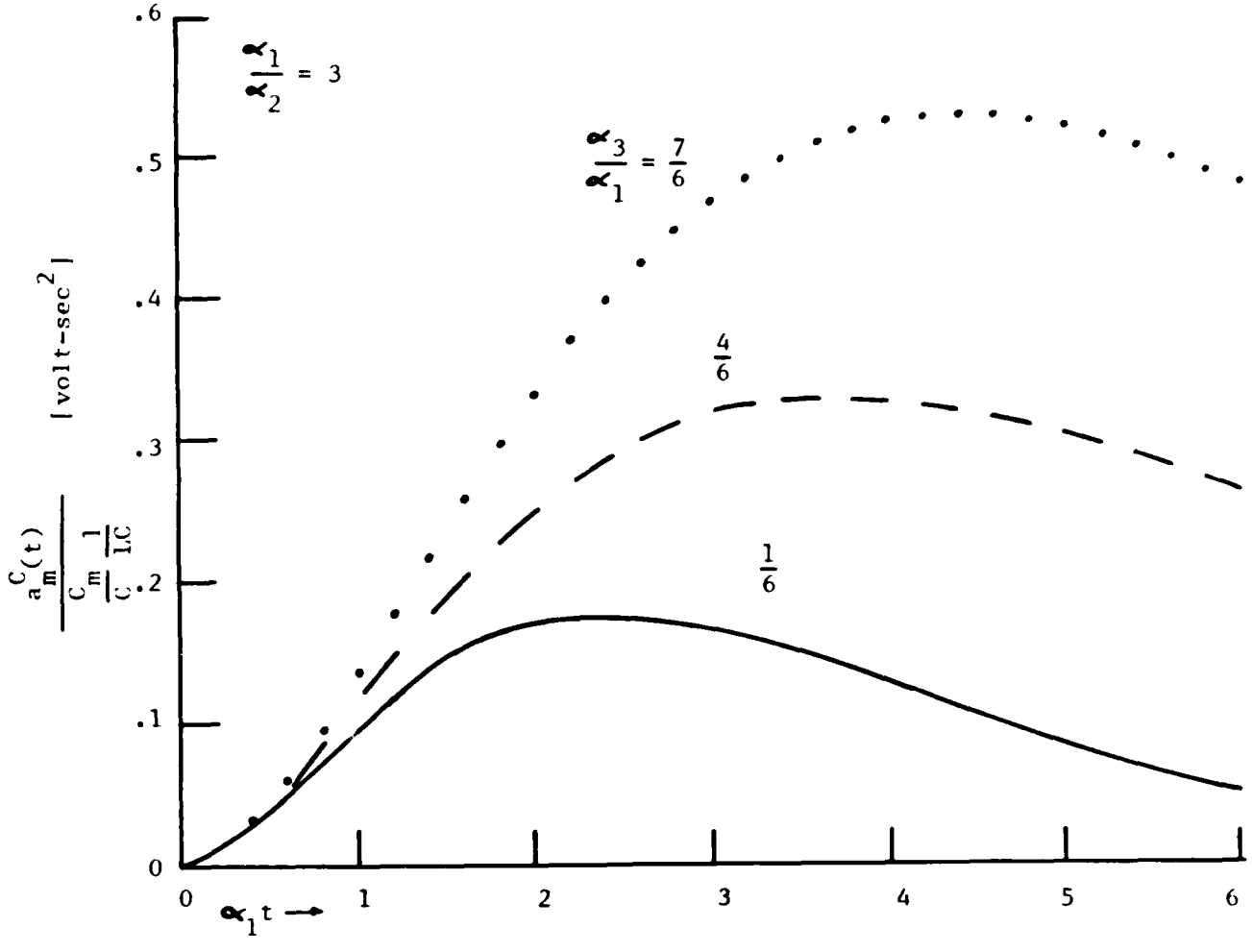

Fig. 7.6. Normalized capacitively coupled cross step responses vs. normalized time.

$$(\alpha_2 - \alpha_1)^2 = (\alpha_1 - \alpha_2)^2 = \left(\frac{R}{L} + \frac{1}{R_o C}\right)^2 - \frac{4}{LC}\left(1 + \frac{R}{R_o}\right). \tag{7.21}$$

The maximum value of the step response can be estimated to be of the order,

$$a_m{}^C(t)_{max} \cong \frac{C_m}{C} \cdot \frac{1}{LC} \cdot \frac{1}{(\alpha_1 - \alpha_2)^2},$$

$$\cong \frac{C_m}{C} \cdot \frac{1}{LC} \cdot \frac{1}{\left(\frac{R}{L} + \frac{1}{R_o C}\right)^2 - \frac{4}{LC}\left(1 + \frac{R}{R_o}\right)}. \tag{7.22}$$

It is interesting to compare this last result with the previously calculated value of mid-band gain (7.3) which was,

$$\left.\frac{V_m(s)}{V_{in}(s)}\right|_{midband} \cong \frac{C_m}{C} \cdot \frac{1}{LC} \cdot \frac{1}{(\alpha_1 + \alpha_2)^2},$$

$$\cong \frac{C_m}{C} \cdot \frac{1}{LC} \cdot \frac{1}{\left(\frac{R}{L} + \frac{1}{R_o C}\right)^2}. \tag{7.23}$$

To minimize capacitive coupling, these last two time-domain and frequency-domain expressions imply that the product,

$$P_C = \frac{C_m}{C} \cdot \frac{1}{LC} \cdot \frac{1}{\left(\frac{R}{L} + \frac{1}{R_o C}\right)^2}, \tag{7.24}$$

should be made as small as possible. If $R/L >> 1/(R_o C)$ then this product simplifies to,

$$P_C = \frac{C_m}{C} \cdot \frac{L/R}{RC}, \tag{7.25}$$

which has the interesting interpretation of C_m/C times the ratio of the L/R time constant to the RC time constant. To minimize P_C reduce C_m/C, the ratio of mutual capacitance to line capacitance, decrease the L/R time constant, and increase the RC time constant. The product P_C can also be written as,

$$P_C = \frac{C_m L}{R^2 C^2}, \tag{7.26}$$

and this suggests that, for both fixed path ohmic loss (or heating) and mutual capacitance C_m, path capacitance should be increased and path inductance decreased to reduce capacitive coupling.

To denote inductive coupling the notation $V_m(s) = V_m{}^L(s)$ is used in Fig. 7.2. The voltage transfer function $V_m{}^L(s)/V_{in}(s)$ can be evaluated by assuming that the current I(s) in the lower path is insignificantly influenced by I'(s), the current induced in the upper path due to mutual inductance L_m. Also, the mutual capacitance C_m is ignored. Under these assumptions, the voltage transfer function is,

$$\frac{V_m{}^L(s)}{V_{in}(s)} = -\frac{L_m}{L} \cdot \frac{1}{LC} \cdot \frac{s(1 + sR_oC)/(R_oC)}{\left\{s^2 + s\left(\frac{R}{L} + \frac{1}{R_oC}\right) + \frac{1}{LC}\left(1 + \frac{R}{R_o}\right)\right\}^2}. \tag{7.27}$$

The voltage transfer function (7.27) is bandpass with maximum mid-frequency gain given by,

$$\frac{V_m{}^L(s)}{V_{in}(s)} \cong \frac{-L_m}{L} \cdot \frac{1}{LC} \cdot \frac{1}{\left(\frac{R}{L} + \frac{1}{R_oC}\right)^2}. \tag{7.28}$$

At very high frequencies the gain rolls off at -12 dB/octave and has the general form,

$$\frac{V_m^L(s)}{V_{in}(s)} \cong \frac{-L_m}{L} \cdot \frac{1}{LC} \cdot \frac{1}{s^2}. \tag{7.29}$$

At low frequencies the gain rises at +6 dB/octave and takes the form,

$$\frac{V_m^L(s)}{V_{in}(s)} \cong -sL_m \frac{1}{R_o\left(1 + \frac{R}{R_o}\right)^2}. \tag{7.30}$$

These results show that, for fixed path parameters R, L, and C, inductive coupling is reduced when either the mutual inductance L_m and/or load resistance R_o is decreased. When path parameters are adjustable, inductive coupling is reduced by increasing the path inductance L, keeping mutual inductance fixed, so that the ratio L_m/L decreases.

Transient responses can be derived from the general voltage transfer function (7.27) by inverse Laplace transformation. As before, the coupled voltage when the input is an impulse h(t) or unit step u(t) is evaluated. These coupled voltages (or cross impulse and step responses) are denoted by $h_m^L(t)$ and $a_m^L(t)$, respectively. Knowing the impulse response, the coupled response to an arbitrary input voltage waveform can be evaluated by temporal convolution. The step response yields the actual time-domain waveform of the coupled voltage due to a typical step transition of a logic sequence.

The impulse response $h_m^L(t)$ is the inverse Laplace transform of the voltage transfer function (7.17) which can be rewritten as,

$$\frac{V_m^L(s)}{V_{in}(s)} = \frac{-L_m}{L} \cdot \frac{1}{LC} \cdot \frac{s(s + \alpha_4)}{(s + \alpha_1)^2(s + \alpha_2)^2}, \tag{7.31}$$

where,

$$\alpha_4 = 1/(R_o C), \tag{7.32}$$

and α_1 and α_2 the same as for capacitive coupling and given by (7.7) and (7.8). Using a partial fraction expansion and performing termwise inverse Laplace transformation, in the same way as for capacitive coupling, the coupled impulse response due to inductive coupling has the general form,

$$h_m^L(t) = \frac{-L_m}{L} \cdot \frac{1}{LC} \left(a_3 + b_3 t\right)e^{-\alpha_1 t} + \left(c_3 + d_3 t\right)e^{-\alpha_2 t}, \tag{7.33}$$

where the constants a_3 through d_3 are,

$$a_3 = \frac{\alpha_4(\alpha_1 + \alpha_2) - 2\alpha_1\alpha_2}{(\alpha_2 - \alpha_1)^3}, \tag{7.34}$$

$$b_3 = -\alpha_1 \frac{(\alpha_4 - \alpha_1)}{(\alpha_2 - \alpha_1)^2}, \tag{7.35}$$

$$c_3 = \frac{\alpha_4(\alpha_1 + \alpha_2) - 2\alpha_1\alpha_2}{(\alpha_1 - \alpha_2)^3}, \tag{7.36}$$

$$d_3 = -\alpha_2 \frac{(\alpha_4 - \alpha_2)}{(\alpha_1 - \alpha_2)^2}. \tag{7.37}$$

No curves of the cross impulse response (7.33) need be plotted because they are identical to those in Figs. 7.3 and 7.4 when the substitutions $-L_m/L \rightarrow C_m/C$ and $\alpha_4 \rightarrow \alpha_3$ are made. To verify these substitutions compare (7.33) to (7.11). Note, however, that the polarity of the inductive cross impulse response is inverted relative to the capacitive

cross impulse response.

The coupled step response due to inductive coupling has the form

$$a_m{}^L(t) = \frac{-L}{L_m} \cdot \frac{1}{LC} \left\{ (a_4 + b_4 t)e^{-\alpha_1 t} + (C_4 + d_4 t)e^{-\alpha_2 t} \right\}, \tag{7.38}$$

where the constants a_4 through d_4 are,

$$a_4 = \frac{\alpha_2 + \alpha_1 - 2\alpha_4}{(\alpha_2 - \alpha_1)^3}, \tag{7.39}$$

$$b_4 = \frac{\alpha_4 - \alpha_1}{(\alpha_2 - \alpha_1)2}, \tag{7.40}$$

$$c_4 = \frac{\alpha_2 + \alpha_1 - 2\alpha_4}{(\alpha_1 - \alpha_2)^3}, \tag{7.41}$$

$$d_4 = \frac{\alpha_4 - \alpha_2}{(\alpha_1 - \alpha_2)^2}. \tag{7.42}$$

As with the cross impulse responses, the cross step responses for inductive coupling can be seen in Figs. 7.5 and 7.6 with the substitutions $-L_m/L \rightarrow C_m/C$ and $\alpha_4 \rightarrow \alpha_3$. Again, polarity is reversed.

Similar to capacitive coupling, the denominator of each term in (7.23) has the constant factor,

$$(\alpha_2 - \alpha_1)^2 = (\alpha_1 - \alpha_2)^2 = \left(\frac{R}{L} + \frac{1}{R_o C}\right)^2 - \frac{4}{LC}\left(1 + \frac{R}{R_o}\right). \tag{7.43}$$

This implies that the maximum value of the step response can be estimated to be of the order,

$$a_m{}^L(t)\Big|_{max} \cong \frac{-L_m}{L} \cdot \frac{1}{LC} \cdot \frac{1}{(\alpha_1 - \alpha_2)^2},$$

$$\frac{-L_m}{L} \cdot \frac{1}{LC} \cdot \frac{1}{\left(\frac{R}{L} + \frac{1}{R_o C}\right)^2 - \frac{4}{LC}\left(1 + \frac{R}{R_o}\right)}. \qquad (7.44)$$

This last result can be compared with the previously calculated midband gain (7.28) which was,

$$\frac{V_m{}^L(s)}{V_{in}(s)}\Bigg|_{midband} \cong \frac{-L_m}{L} \cdot \frac{1}{LC} \cdot \frac{1}{(\alpha_1 + \alpha_2)^2}$$

$$\cong \frac{-L_m}{L} \cdot \frac{1}{LC} \cdot \frac{1}{\left(\frac{R}{L} + \frac{1}{R_o C}\right)^2}. \qquad (7.45)$$

To minimize inductive coupling, these last two time-domain and frequency-domain expressions imply that the product,

$$P_L = \frac{L_m}{L} \cdot \frac{1}{LC} \cdot \frac{1}{\left(\frac{R}{L} + \frac{1}{R_o C}\right)^2}, \qquad (7.46)$$

generally should be made as small as possible. If $R/L >> 1/(R_o C)$ then this product simplifies to,

$$P_L = \frac{L_m}{L} \cdot \frac{L/R}{RC}, \qquad (7.47)$$

which is the product of L_m/L and the ratio of the L/R time constant to the RC time constant. The product P_L can also be written as,

$$P_L = \frac{L_m}{R^2 C}. \tag{7.48}$$

and this suggests that, for both fixed path ohmic loss (or heating) and mutual inductance L_m, path capacitance should be increased to reduce inductive coupling.

The conclusion based on the foregoing analysis of the coupling model is that there are several options available to reduce coupling and interference in integrated circuit signal paths: (1) increase path capacitance; (2) decrease mutual capacitance and mutual inductance; (3) increase path loading; (4) if ohmic losses and heating are not critical, increase path resistance. Option (1), increasing path capacitance, appears most promising. This can be accomplished by increasing the relative dielectric of the substrate and/or reducing the thickness of the substrate layer.

8. Field-Theoretic Path Coupling Model

An important type of electric circuit consists of conducting paths on a dielectric sheet that is bounded on one side by air, and on the other side by a conducting plane. This is the case for the majority of chip area in an integrated circuit because of the many interconnections. The interaction of circuit elements on such a structure includes not only the conducting paths but also the coupling due to electromagnetic waves that are generated and travel in and along the surface of the dielectric. This is particularly important where extremely high frequencies are present due to very high clocking rates. It is well known that a dielectric-coated metal plane supports a surface wave that propagates in the dielectric. However, such surface waves are usually derived as possible solutions of Maxwell's equations when the conditions of a surface wave are imposed (viz., that the surface wave be exponentially attenuated in the air in the direction perpendicular to the dielectric). It is not obvious that such a wave is, in fact, generated by alternating currents located on the air-dielectric boundary. A first step in the determination of the fields generated by such currents is a complete analysis of the electromagnetic field of a unit infinitesimal horizontal dipole (i.e., an infinitely small conductor with an electric current moment $Ih_e = 1$ ampere-meter) located on the air-dielectric surface as shown in Fig. 8.1.

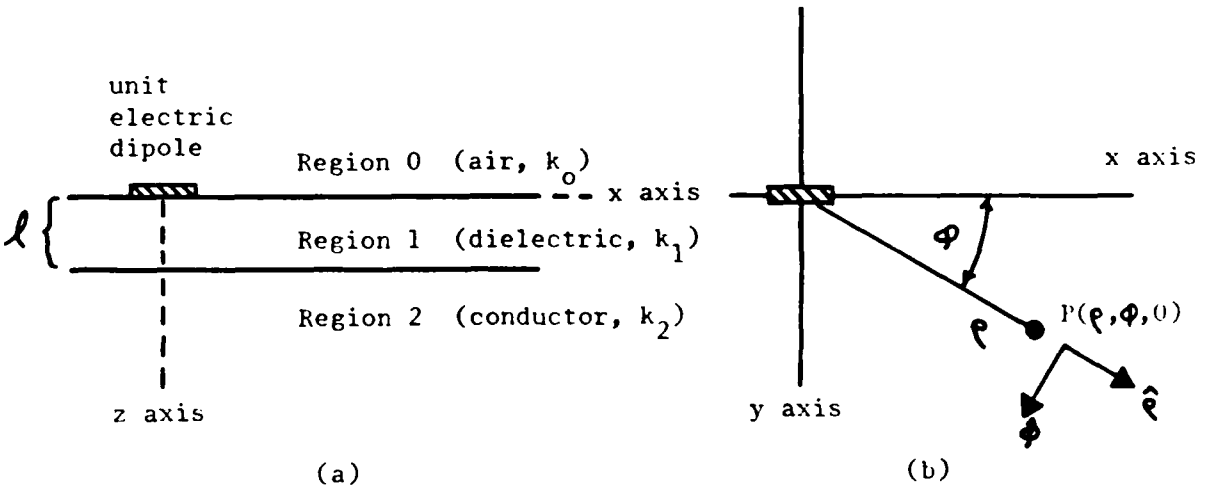

Fig. 8.1(a) Side view of unit electric dipole on plane boundary $z = 0$ between air and a dielectric; (b) Top view of unit electric dipole on dielectric surface and observation point $P(\rho, \varphi, 0)$ where the ρ and φ components of the electric field vector are to be evaluated.

Once this is known, the fields generated by conductors of finite length can be derived. These include single conductors, parallel conductors forming a transmission line, and various circuits with small lumped elements.

The electromagnetic field generated by a unit dipole when on the boundary between air (Region 0, $z \leq 0$) and a dielectric or conducting half-space (Region 1, $z \geq 0$) is well known. The radial component of the electric field $E_{1\ell}(\rho, \varphi, 0)$ includes a wave of the type known as a lateral wave which travels in the air along the boundary and a direct wave that travels in the adjacent half-space. The lateral wave in Region 0 has the coefficient $e^{ik_0\rho}$ with associated amplitude factors, the direct wave in Region 1 has the coefficient $e^{ik_1\rho}$ with associated amplitude factors. Because the wavenumber k differs, these two waves propagate at different velocities. Unfortunately, these known formulas for the air-dielectric interface are not valid for a three-layered region, like an integrated circuit.

Corresponding new formulas were derived for the horizontal electric dipole on the boundary of a three-layered region shown in Fig. 8.1. The mathematical details are too lengthy to be presented in this report and will be published elsewhere. Only the major research results and their relevance to the coupling/interference problem in very-high-speed integrated circuits are discussed here.

The following practical approximations were used to derive the new formulas for the fields:

$$|k_0^2| << |k_1^2| << |k_2^2|, \quad |k_1 \ell| < 1, \tag{8.1}$$

where the wavenumber,

$$k_j = \beta_j + i\alpha_j = \omega[\mu_0(\epsilon_j + i\sigma_j/\omega)]^{1/2}, \tag{8.2}$$

and $\omega = 2\pi f$, the radian frequency. In (8.2) the quantities μ_0, ϵ, and σ have their usual meanings. In (8.1), $|k_1 \ell|$ is interpreted as the electrical thickness of the dielectric layer whose physical thickness is ℓ.

The general form for the radial electric field at the air-dielectric surface due to a horizontal electric dipole (see Fig. 8.1) is,

$$E_{1\rho}(\rho, \phi, 0) = \frac{\omega\mu_o}{2\pi k_1^2}\cos\phi\left\{2e^{ik_1\rho}\left[\frac{k_1}{\rho^2}\left(1 - i\frac{k_1}{k_2}\right) + \frac{i}{\rho^3}\left(1 - i\frac{k_1}{2k_2}\right)\right]\right.$$

$$+ e^{ik_o\rho}\left(\frac{ik_1}{k_2\rho^3}\right) \qquad (8.3)$$

$$\left. + ik_1\ell\left[e^{ik_o\rho}\left(\frac{ik_o^2}{\rho} - \frac{k_o}{\rho^2} - \frac{i}{\rho^3}\right) - e^{ik_1}\left(\frac{ik_1}{\rho^2} - \frac{1}{2\rho^3}\right)\right]\right\}$$

This includes contributions from a surface wave that travels in the dielectric region 1 with the propagation factor $e^{ik_1\rho}$ and a lateral wave that travels along the surface in the air with the propagation factor $e^{ik_o\rho}$. These two waves have different velocities of propagation.

The quasi-static or near field part of (8.3) is,

$$E_{1\rho}(\rho, \phi, 0) \sim \frac{\omega\mu_o}{2\pi k_1^2}\frac{\cos\phi}{\rho^3}\left[2i + \frac{k_1}{k_2}(1 + i) + k_1\ell\,(1 + i/2)\right]. \qquad (8.4)$$

At large distances, the lateral wave dominates and,

$$E_{1\rho}(\rho, \phi, 0) \sim \frac{-\omega\mu_o k_o^2\ell}{2\pi k_1}\frac{e^{ik_o\rho}}{\rho}, \quad k_o\rho > 1. \qquad (8.5)$$

The general form for the phi component of the electric field at the air-dielectric interface due to a horizontal electric dipole (see Fig. 8.1) is,

$$E_{1\phi}(\rho, \varphi, 0) = \frac{-\omega\mu_o}{2\pi k_1^2} \sin\varphi \left\{ e^{ik_1\rho} \left[\frac{ik_1^2}{\rho} - \frac{k_1}{\rho^2} - \frac{i}{\rho^3} \right] \right. \tag{8.6}$$

$$\left. -ik_1\ell \left[2e^{ik_o\rho} \left(\frac{k_o}{\rho^2} + \frac{i}{\rho^3} \right) + e^{ik_1\rho} \left(\frac{k_1^2}{\rho} + \frac{ik_1}{2\rho^2} \right) \right] \right\}.$$

The quasi-static or near-field part of (8.6) is,

$$E_{1\phi}(\rho, \varphi, 0) \sim \frac{i\omega\mu_o}{2\pi k_1^2} \frac{\sin\varphi}{\rho^3} [1 + 2ik_1\ell], \quad |k_1\rho|^2 << 1. \tag{8.7}$$

At large distances the far field has the form,

$$E_{1\phi}(\rho, \varphi, 0) \sim \frac{-i\omega\mu_o}{2\pi} \sin\varphi \frac{e^{ik_1}}{\rho} [1 - k_1\ell], \quad |k_1\rho|^2 << 1. \tag{8.8}$$

Although the general formulas for the components of the electric field, (8.3) and (8.6), are complicated, some important observations relevant to coupling and interference in integrated circuits can be made. First, reducing electric field strength in the region near the current element is desireable because coupling and interference are proportionally reduced. The near field terms in (8.4) and (8.7) each have the coefficient,

$$\frac{\omega}{k_1} = \frac{1}{[\mu_o(\epsilon_1 + i\sigma_1/\omega)]^{1/2}}. \tag{8.9}$$

Therefore, increasing the permittivity ϵ_1 of the dielectric layer reduces field strength (and, consequently, coupling and interference with nearby conductors and circuits). At high frequencies σ_1/ω becomes smaller tending to increase field strength. Increasing the conductivity of the dielectric layer to compensate this may be a poor choice because

signal losses in the dielectric will increase and heating could be problematic.

At larger distances away from the current element the lateral wave has the coefficient,

$$\frac{\omega k_o^2 \ell}{k_1} = \frac{k_o^2 \ell}{[\mu_o(\epsilon_1 + i\sigma_1/\omega)]^{1/2}}. \tag{8.10}$$

Again, field strength is reduced by increasing the dielectric's permittivity ϵ_1. Coupling and interference also can be reduced at larger distances from the current element by reducing the physical thickness ℓ of the dielectric layer as can be seen from (8.10). Because k_o^2 appears in the numerator of (8.10), increasing k_o would proportionally increase the strength of the lateral wave and coupling or interference due to it. This means that using a material with $\epsilon > \epsilon_o$ in place of air in Region 1 is not good from the standpoint of interference/coupling due to the lateral wave.

The general expression for the radial electric field contains several $1/k_2$ terms which can be made smaller by increasing the conductivity σ_2 of the ground plane as can be inferred from the relation,

$$k_2 = \omega[\mu_o(\epsilon_2 + i\sigma_2/\omega)]^{1/2}. \tag{8.11}$$

In summary, from the field-theoretic path coupling model based on a study of fields generated by a horizontal current moment parallel to the air-dielectric surface of the three-layered problem, coupling and interference generally can be minimized by: (1) <u>increasing the permittivity ϵ_1 of the dielectric layer</u>; (2) <u>decreasing the thickness ℓ of the dielectric layer</u>; (3) <u>increasing the conductivity of the ground plane below the dielectric layer</u>. These results are consistent with that from the previous section, namely, increase path capacitance to minimize coupling and interference.

The interesting new research result in this section is the existence of two mechanisms of coupling from a current moment on the

dielectric surface: one due to a lateral wave and the other due to a surface wave. Because the velocity of propagation of one wave is different from the other, these interfering signals arrive at some point on the surface of the dielectric at different times. This may be critical at very high clocking rates.

END

2-87

DTIC